

Quantitative model for gene regulation by λ phage repressor

(gene regulation/repressors and operators/cooperative interaction/thermodynamic model)

GARY K. ACKERS*, ALEXANDER D. JOHNSON^{†‡}, AND MADELINE A. SHEA*

*Department of Biology and McCollum-Pratt Institute, The Johns Hopkins University, Baltimore, Maryland 21218; and [†]The Biological Laboratories, Harvard University, Cambridge, Massachusetts 01238

Communicated by Mark Ptashne, November 6, 1981

ABSTRACT A statistical thermodynamic model has been developed to account for the cooperative interactions of the bacteriophage λ repressor with the λ right operator. The model incorporates a general theory for quantitatively interpreting cooperative site-specific equilibrium binding data. Values for all interaction parameters of the model have been evaluated at 37°C, 0.2 M KCl, from results of DNase protection experiments *in vitro* [A. D. Johnson, B. J. Meyer, & M. Ptashne, *Proc. Natl. Acad. Sci. USA* (1979) 76, 5061–5065]. With these values, the model predicts repression curves at the divergent promoters P_R and P_{RM} that control transcription of genes coding for the regulatory proteins *cro* and repressor, respectively. At physiological repressor concentrations, repression at P_R is predicted to be nearly complete whereas P_{RM} is predicted to remain highly active. The results demonstrate the importance of cooperative interactions between repressor dimers bound to the adjacent operator sites O_{R1} and O_{R2} in maintaining a stable lysogenic state and in allowing efficient switchover to the lytic state during induction.

In prokaryotes, genes are commonly switched on and off by the interactions of regulatory proteins with specific DNA sequences. A particularly complex example of such a switch is found at the right operator (O_R) of bacteriophage λ : this operator consists of three tandem DNA sites that are recognized by two phage-encoded regulatory proteins (the λ repressor and *cro* protein). When phage λ is in the “lysogenic state,” the λ repressor (*cl* gene product) is synthesized and occupies sites O_{R1} and O_{R2} . In this configuration of O_R , the *cro* gene is repressed and the *cl* gene is transcribed.

The phage switches into the “lytic state” when the repressor protein is cleaved in half by the *recA* protein, an action initiated by DNA damage. As repressor is destroyed, the *cro* gene is derepressed and the *cro* protein is made and occupies site O_{R3} , turning off transcription of the *cl* gene, yet allowing its own synthesis. In this fashion, the phage can switch from one state (lysogeny) to another (lytic growth) in response to an external signal (for review, see ref. 1).

In this paper, we consider the lysogenic state (repressor on, *cro* off) in an attempt to understand the physical principles that govern the ways in which the protein–DNA and protein–protein interactions operate in concert to produce the known physiological behavior. We show that a model based on statistical thermodynamic assumptions is sufficient to account for some of the known physiological properties of the repressor–operator regulatory system. A brief summary of certain aspects of this work has been presented elsewhere (1).

Models for interactions at the *lac* operon have been developed to include effects of inducer and nonspecific DNA on the

binding of *lac* repressor (2–4). The systems of λ and other inducible phages differ from *lac* by using multiple operator binding sites that have cooperative interactions between bound repressors (1). This requires a more elaborate theoretical approach to the protein–DNA binding problem—one that has not previously been developed.

The mathematical model we present here incorporates a set of rules and assumptions derived from previous genetic, biochemical, and structural studies. Combination of this information with statistical thermodynamic assumptions generates a quantitative formulation that incorporates salient features of the qualitative description developed over the last several years (1, 5–9). This quantitative model has the following significance. (i) It provides a way to test assumptions regarding the physical bases for operation of the system. Thus, it predicts quantitatively the activities of the two O_R -controlled promoters (P_R and P_{RM}) as a function of repressor concentration, and these predictions can then be compared with known physiological properties of the system. (ii) It points out features of the λ operator system that were not obvious (or at least fully appreciated) from previous experiments. (iii) It incorporates a theory for interpreting cooperative site-specific equilibrium binding data (e.g., from protection-method experiments) that should be applicable to other regulatory systems. Based primarily on the results of *in vitro* DNase I protection experiments, we have generated a complete and unique evaluation of the free energies for the system at 37°C, 0.2 M KCl, conditions that may resemble “physiological” (10).

THE SYSTEM

We consider the following interacting components (Fig. 1): (i) the λ right operator containing the 17-base pair binding sites O_{R1} , O_{R2} , and O_{R3} , (ii) active repressor dimers capable of binding tightly to the operator sites, and (iii) monomers that cannot bind to DNA but can associate to form active dimers. We wish to calculate (i) the probability that an operator template will exist in a given microscopic configuration (e.g., with O_{R1} and O_{R3} occupied and O_{R2} vacant) and (ii) the probabilities of certain configurations of repressor molecules bound to the operator that have biological significance (e.g., the total probability that O_{R3} is occupied by repressor, obtained by summing all the ways this can occur). The following assumptions and definitions provide a basis for these calculations.

Assumptions[§] and Definitions. 1. We assume that occupancy of operator sites by repressor dimers and the resulting effects

[†] Present address: Department of Biochemistry and Biophysics, University of California, San Francisco, CA 94143.

[§] Several of these premises (notably 2, 3, 5, and 6) must be regarded as “facts.” They are designated here as “assumptions” solely to indicate their formal role in the mathematical model.

The publication costs of this article were defrayed in part by page charge payment. This article must therefore be hereby marked “advertisement” in accordance with 18 U. S. C. §1734 solely to indicate this fact.

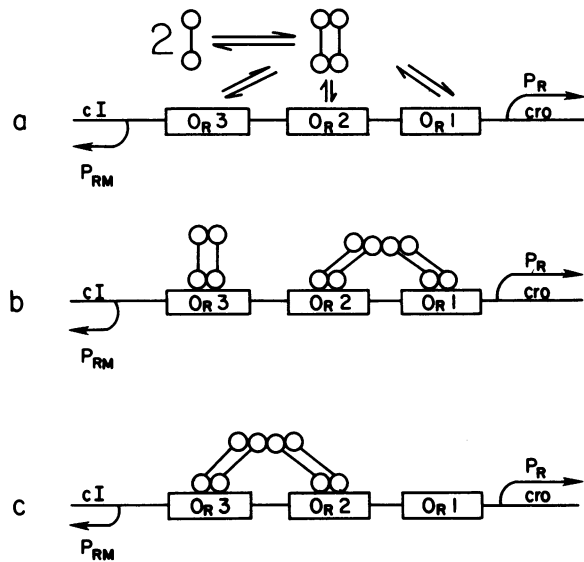


FIG. 1. Interactions of repressor molecules (○—○) at the right operator, O_R , of the λ phage genome. The DNA binding sites for repressor (designated O_{R1} , O_{R2} , and O_{R3}) are each composed of 17 base pairs and are separated by spacers of 6 and 7 base pairs. Binding of repressor molecules controls transcription by RNA polymerase from the two divergent promoters, P_R and P_{RM} . Transcription of the *cro* gene from P_R and consequent synthesis of *cro* protein leads to lytic growth of the phage genome and cell lysis. Transcription of the *cl* gene from the promoter P_{RM} and consequent synthesis of repressor is required to maintain the lysogenic state by preventing *cro* synthesis. (a) Active repressor dimers in equilibrium with inactive monomers. The dimers bind reversibly to each of the three operator sites (arrows). Binding can result in any of the seven combinations shown in Table 1. (b and c) Types of cooperative interaction believed to occur between adjacent bound repressors (configurations 7 and 8 of Table 1).

on gene transcription are determined by equilibrium statistical thermodynamic probabilities. The probabilities arise from (i) the free energies of binding repressor dimers to the specific operator sites, (ii) the free energies of interaction between repressor molecules bound to adjacent operator sites, (iii) the free energy of repressor dimer assembly from monomers, and (iv) the concentrations of the interacting components.

2. Repressor dimers bound simultaneously to adjacent operator sites O_{R1} and O_{R2} interact with each other (6). We define the free energy of cooperative interaction ΔG_{12} as the difference between the free energy required to fill the two sites simultaneously and the sum of the energies required to fill them individually.

3. Repressor dimers may similarly bind simultaneously to the adjacent operator sites O_{R2} and O_{R3} in a cooperative manner (6); the free energy of this cooperative interaction is ΔG_{23} .

4. Cooperative interaction between adjacent bound repressors at O_{R2} and O_{R3} occurs only when O_{R1} is vacant. When O_{R1} is occupied, occupancy of O_{R3} occurs with the same energy whether O_{R2} is occupied or vacant (7).

5. Transcription of the *cro* gene from P_R is turned off on templates in which repressor dimers occupy O_{R1} , O_{R2} , or both (7–9).

6. A repressor dimer bound to O_{R3} is necessary and sufficient to turn off the promoter P_{RM} responsible for transcription of the repressor gene *cl* (7–9).

7. In mutant operators in which one or more sites are incapable of binding repressor appreciably, the intrinsic interactions at the remaining sites are unaltered (6).

Microscopic Configurations and Energy States. Assumptions 2, 3, and 4 define a set of eight possible structures (i.e.,

Table 1. Microscopic configurations and free energies for the operator–repressor system O_R^+

Species (s)	Configuration			Free energy contributions	Total free energy (ΔG_s), kcal*
	O_{R3}	O_{R2}	O_{R1}		
1	O	O	O	Reference state	0
2	O	O	R	ΔG_1	-11.7
3	O	R	O	ΔG_2	-10.1
4	R	O	O	ΔG_3	-10.1
5	O	R ↔ R		$\Delta G_1 + \Delta G_2 + \Delta G_{12}$	-23.8
6	R	O	R	$\Delta G_1 + \Delta G_3$	-21.8
7	R ↔ R	O		$\Delta G_2 + \Delta G_3 + \Delta G_{23}$	-22.2
8	R	R ↔ R		$\Delta G_1 + \Delta G_2 + \Delta G_3 + \Delta G_{12}$	-33.9

Individual operator sites are denoted by O if vacant or R if occupied by a bound repressor dimer. ↔, Pairwise interaction between adjacent bound repressors. ΔG_s represents the standard free energy of formation relative to the reference template ($s = 1$) for each operator species s . ΔG_1 , ΔG_2 , and ΔG_3 are intrinsic free energies for binding repressor dimers to the various sites and are each related to a corresponding equilibrium constant K_i by the standard relationship $\Delta G_i = -RT \ln K_i$ ($i = 1, 2, \text{ or } 3$).

* 1 cal = 4.18 J.

microscopic configurations of operators) that are assumed to have sufficiently high probability to warrant consideration. Table 1 lists the free energy terms contributing to the various configurations of the operators. The magnitudes and relative values of these interaction energies were determined from experimental results (see below).

Mathematical Relationships of the Model. For each of the eight microscopic configurations of Table 1, we can formulate an exact expression of its probability as a function of repressor concentration according to the principles of statistical thermodynamics. The probability of an operator in the s configuration can be written (cf. ref. 11) as

$$f_s = \frac{\exp(-\Delta G_s/RT) [R_2]^j}{\sum_{sj} \exp(-\Delta G_s/RT) [R_2]^j}, \quad [1]$$

where ΔG_s is the relative free energy of the s configuration (Table 1), R is the gas constant, T is the absolute temperature, $[R_2]$ is the concentration of unbound repressor dimers, and j is the number of repressor dimers bound to an operator in the s configuration. The summation of s is taken from 0 through 8 and j has the values (0, 1, 2, 3) appropriate to the species s . The probability f_s represents the fraction of operators that, at a given concentration of unbound repressor dimers $[R_2]$, will have the configuration whose free energy is ΔG_s .

Once the probabilities for each of the eight operator states are known, we can describe the binding of repressor to each operator site in the full cooperative system. For example, the total occupancy of O_{R3} is given by

$$f_{O_{R3}} = f_4 + f_6 + f_7 + f_8 = f_{PRM}. \quad [2]$$

Note that, by assumption 5, this is also the fraction f_{PRM} of templates in which P_{RM} is repressed. Likewise (by assumption 4) the fraction of P_R -repressed templates is

$$f_{PR} = f_2 + f_3 + f_5 + f_6 + f_7 + f_8. \quad [3]$$

Eqs. 1–3 provide a statistical thermodynamic translation of the model assumptions into the biologically significant quantities f_{PR} and f_{PRM} . Thus far, our equations are expressed in terms of the interaction free energies of Table 1 and the concentration

of unbound repressor dimers $[R_2]$. To relate these quantities to the total concentration of repressors (R_t), we note that

$$[R_t] = [R_1] + 2[R_2] + 2[O_i] \sum j f_j, \quad [4]$$

where $[R_1]$ is the concentration of repressor monomers (which cannot bind DNA, see above) and $[O_i]$ is the total concentration of operators. Eqs. 1–4 plus the equation for dimer formation ($[R_2] = K_d[R_1]^2$) (12) comprise the mathematical formulation of the model. This provides us with the means to predict the P_R and P_{RM} repression curves, f_{PR} and f_{PRM} , as a function of repressor concentration, once the interaction free energies are known.

EVALUATION OF THE INTERACTION PARAMETERS

Having set up the formal model, we now consider the values for the five free energy terms of Table 1 (ΔG_1 , ΔG_2 , ΔG_3 , ΔG_{12} , and ΔG_{23}). From the DNase protection experiments of Johnson *et al.* (6), the concentration of repressor dimers required for half saturation of the individual operator sites has been determined for the wild-type operator and for mutant operators in which one or two of the three repressor binding sites have been destroyed by point mutation and deletion. To calculate the five free energy terms from these data, we use the following expressions for occupancy of the three sites in wild-type operators:

$$f_{OR1} = f_2 + f_5 + f_6 + f_8 \quad [5]$$

$$f_{OR2} = f_3 + f_5 + f_7 + f_8 \quad [6]$$

$$f_{OR3} = f_4 + f_6 + f_7 + f_8. \quad [7]$$

For the mutant operators, the probabilities have similar form, each containing the appropriate combinations of terms. Each of the 11 data points (Table 2) gives a value of R_2 at which the individual binding site is half occupied; thus, each of these data points defines an equation of the form shown above for which $f_{site} = 0.5$. The system of 11 simultaneous equations was then solved by a nonlinear least-squares procedure (13) that estimates the best values for the five energies (ΔG_1 , ΔG_2 , ΔG_3 , ΔG_{12} , ΔG_{23}) and the confidence limits associated with each value. Results of these calculations (performed on a Hewlett-Packard 1000 system) are given in Table 3.

The effects of experimental uncertainty in repressor concentration (as high as 30% random error) were explored. Such errors were found to cause changes of only a few tenths of a kilocalorie in the energies resolved from the 11 simultaneous equations. A full treatment of the numerical analysis of these and similar data will be presented elsewhere.

PREDICTED BEHAVIOR OF THE SYSTEM

Repression Curves at P_R and P_{RM} . Having resolved the five free energies that define the operator–repressor interactions

Table 2. Values of $[R_2]$ for half occupation of individual sites

DNA Template	DNA		
	O _R 3	O _R 2	O _R 1
O _R ⁺ (wild type)	25	2	1
O _R 1 ⁻	5	5	—
O _R 2 ⁻	25	—	2
O _R 1 ⁻ , O _R 2 ⁻	25	—	—
O _R 1 ⁻ , O _R 3 ⁻	—	25	—
O _R 3 ⁻	—	2	1

Data are from DNase protection titrations in units of 3 nM. All results are from ref. 6 except that for O_R3⁻.

Table 3. Resolved interaction free energies for O_R

	Energy, kcal
Individual site binding	
ΔG_1	-11.69 ± 0.03
ΔG_2	-10.10 ± 0.05
ΔG_3	-10.09 ± 0.02
Cooperative interaction	
ΔG_{12}	-1.99 ± 0.06
ΔG_{23}	-1.94 ± 0.06

Results are ±65% confidence limits for estimated values (13).

and using $K_a = 5 \times 10^7 \text{ M}^{-1}$ (12) and $[O_i] = 10^{-9} \text{ M}$ (1), we calculated the repression curves from Eqs. 2–4 for the wild-type operator. The predicted curves are presented in Fig. 2. We note two characteristics of these curves. First, they agree with experimental findings (*in vivo* and *in vitro*) that repressor turns off P_R at lower concentrations than those required to turn off P_{RM} . The curves predict that ≈ 25 -fold more repressor is needed to half repress P_{RM} than to half repress P_R . This value agrees with that determined experimentally *in vitro* by using the abortive initiation assay (14) to measure the activities of the two promoters as a function of repressor concentration (D. Hawley and W. R. McClure, personal communication). In addition, Maurer *et al.* (7) and Meyer and Ptashne (8, 9) have shown *in vivo* that at least 10- to 15-fold more repressor is required to half repress P_{RM} than to half repress P_R . This value was difficult to determine accurately due to the difficulty of measuring low concentrations of repressor *in vivo*.

Second, we note that the predicted P_R and P_{RM} repression curves differ in shape; for example, the P_R curve is steeper. This difference exists because P_R is controlled by two operator sites to which repressor binds cooperatively whereas P_{RM} is controlled by single site. Hawley and McClure (using the abortive initiation assay) have shown that P_R turnoff is, in fact, a steeper function of repressor concentration than is P_{RM} turnoff.

Maintenance of the Lysogenic State. In a lysogen, P_R is very tightly repressed whereas P_{RM} is turned down only $\approx 20\%$ (8). The predicted curves (Fig. 2) are consistent with this finding. For example, at a total repressor concentration of 10^{-7} M , the calculated values of f_{PR} and f_{PRM} are 0.99 and 0.35, respectively. Although the values calculated cannot be taken as an exact rep-

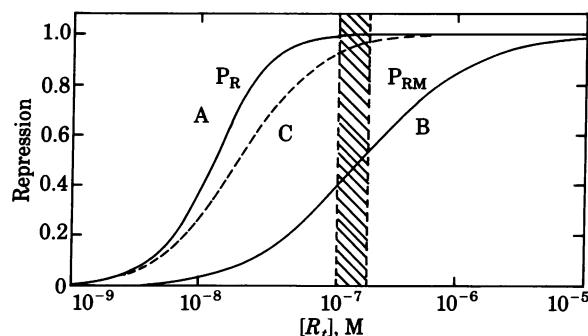


Fig. 2. Predicted repression curves at P_R and P_{RM} . Curve A represents f_{PR} , the probability that an operator template will have O_R1, O_R2, or both occupied (each of these three configurations shuts off transcription from P_R) as a function of R_t in units of monomer. This curve includes all effects of cooperative interaction between repressor dimers bound to adjacent operator sites and also of repressor dimer dissociation into inactive monomers. Curve B represents f_{PRM} , the probability that O_R3 is occupied (required for shutoff of transcription at P_{RM}), including all effects. Curve C, repression curve for P_R devoid of cooperative interactions. \square , Approximate concentration of repressor in a lysogenic cell.

resentation of *in vivo* repression, these curves correctly predict that P_R will be nearly completely repressed while P_{RM} will be highly active. Although the concentration of repressor in a lysogen is not known accurately, it is at least $1-2 \times 10^{-7}$ M (100–200 monomers per cell) (15, 16).

The Importance of Cooperativity. We believe that cooperative interaction between adjacently bound repressor molecules helps to maintain the stability of the lysogenic state and yet allows the phage to be easily induced. First, the cooperativity effectively increases P_R repression at lysogenic concentrations of repressor. This can be seen by comparing the fully cooperative P_R repression curve (A) with the predicted noncooperative repression curve (C) obtained by setting $\Delta G_{12} = \Delta G_{23} = 0$ but not changing ΔG_1 , ΔG_2 , and ΔG_3 . At lysogenic concentrations of repressor (e.g., when P_R is $\approx 20\%$ repressed), the effect of cooperativity is to significantly tighten the repression of P_R . Second, we believe that cooperative repressor binding aids in effectively switching the phage from the lysogenic to the lytic state. Since f_{PR} is a steep function of repressor concentration (Fig. 2), a modest decrease in repressor concentration can lead to a relatively large decrease in extent of repression and a consequent burst of *cro* production.[¶]

Nonspecific DNA Binding. The probability of any configuration of the operator is predicted by Eq. 1. It is determined by the relative free energy of that configuration and the concentration of free repressor dimers in solution. We have tacitly assumed (Eq. 4) that no substantial fraction of the intracellular repressor is sequestered on nonoperator DNA (or other cellular structures). Although we are not certain that this assumption is valid, we do know that, at 0°C in the presence of low (50 mM) salt, the ratio of nonspecific to specific binding for λ repressor is $\approx 10^{-8}$ (12). If this ratio remains the same under "physiological conditions" (37°C, 0.2 M salt; see above), then we estimate that little or none of the repressor in a lysogen is bound to nonoperator DNA (see ref. 1). We emphasize that our theoretical treatment of O_R occupancy by repressor holds irrespective of the degree of nonspecific DNA binding.

DISCUSSION

Several theoretical treatments have been developed to analyze regulatory systems governed by protein–DNA interactions (19–21); however, none of them deal with the problem of interpreting cooperative binding curves at specific nonoverlapping sites. The formulations developed in this study provide a simple rigorous theory to analyze systems of this type. The method can readily be extended to systems other than bacteriophage λ (and its relatives P22 and 434) in which the numbers of binding sites and the rules of interaction and biological function may be different. For example, control of the *Escherichia coli* arabinose operon by *araC* and CAP protein (22, 23), autogeneous regulation of the *E. coli* *lexA* gene (24), and control of the simian virus 40 early genes by the large tumor antigen (25) are all thought to depend on cooperative interactions between adjacent DNA-bound regulatory proteins. The development of DNA sequence analysis and DNase protection methods (26–28) has made possible the generation of individual-site binding data, such as that analyzed here.

In this study, we have shown that a statistical thermodynamic

mechanism for repressor–operator interactions provides a working model that accounts, so far, for certain *in vivo* characteristics of the lysogenic phage. This demonstration of sufficiency of the physical assumptions does not, of course, prove them to be correct or necessary. It is possible that other theories, based for example on purely kinetic mechanisms, could account equally well for the available body of physiological observations.

We believe the present model to be highly credible, however, because it does not depend upon any "adjustment of parameters." Evaluation of the model parameters was carried out independently of their application to *in vivo* situations and was rigorously exact since the interacting components of the *in vitro* binding experiments were at thermodynamic equilibrium. These parameters were then used to predict the *in vivo* behavior of the system. Application of the model to an *in vivo* situation depends on the supposition that the probabilities of interaction will still be governed by their independently determined thermodynamic energies. Evaluation of this assumption can only be obtained by comparing predicted properties with those observed *in vivo*. We found that, without any adjustment of constants, the repression curves and other features predicted by the model are in very good agreement with the physiological observations. This lends credence to the physical assumptions on which the model is based. Further tests of the approach developed here could be carried out by extending the model to include the mutual effects of *cro* and RNA polymerase. These effects, along with dynamic aspects of the system, will be presented in detail elsewhere.

We thank Mark Ptashne for his continuous interest and support in this work. We also thank Benjamin W. Turner, Gary Ketner, William McClure, and Diane Hawley for valuable discussions of the ideas and information described in this paper. This work has been supported by grants from the National Institutes of Health and the National Science Foundation.

1. Johnson, A. D., Poteete, A. R., Lauer, G., Sauer, R. T., Ackers, G. K. & Ptashne, M. (1981) *Nature (London)* **294**, 217–223.
2. von Hippel, P. H., Revzin, A., Gross, C. & Wang, A. C. (1974) *Proc. Natl. Acad. Sci. USA* **71**, 4808–4812.
3. von Hippel, P. H. (1979) in *Biological Regulation and Development*, ed. Goldberger, R. F. (Plenum, New York), pp. 279–347.
4. Dunaway, M., Manly, S. P. & Matthews, K. S. (1980) *Proc. Natl. Acad. Sci. USA* **71**, 7181–7815.
5. Ptashne, M., Jeffrey, A., Johnson, A. D., Maurer, R., Meyer, B. J., Pabo, C. O., Roberts, T. M. & Sauer, R. T. (1980) *Cell* **19**, 1–11.
6. Johnson, A. D., Meyer, B. J. & Ptashne, M. (1979) *Proc. Natl. Acad. Sci. USA* **76**, 5061–5065.
7. Maurer, R., Meyer, B. J. & Ptashne, M. (1980) *J. Mol. Biol.* **138**, 147–161.
8. Meyer, B. J. & Ptashne, M. (1980) *J. Mol. Biol.* **138**, 163–194.
9. Meyer, B. J. & Ptashne, M. (1980) *J. Biol. Biol.* **139**, 195–205.
10. Kao-Huang, Y., Revzin, A., Butler, A. P., O'Conner, P., Noble, D. W. & von Hippel, P. H. (1977) *Proc. Natl. Acad. Sci. USA* **74**, 4228–4232.
11. Hill, T. L. (1960) *Introduction to Statistical Thermodynamics* (Addison Wesley, Reading, MA).
12. Sauer, R. T. (1979) Dissertation (Harvard University, Cambridge, MA).
13. Johnson, M. L., Halvorson, H. R. & Ackers, G. K. (1976) *Biochemistry* **15**, 5363–5371.
14. McClure, W. R. (1980) *Proc. Natl. Acad. Sci. USA* **77**, 5634–5638.
15. Pirrotta, V., Chadwick, R. & Ptashne, M. (1970) *Nature (London)* **227**, 41–44.
16. Bailone, A., Levine, A. & Devoret, R. (1979) *J. Mol. Biol.* **131**, 553–573.

[¶] Bailone *et al.* (16) have shown that, on 90% inactivation of repressor, a lysogen becomes committed to lytic growth. From the repression curve of Fig. 2, we estimate that 90% inactivation leads to $\approx 50\%$ derepression at P_R . Additional calculations (unpublished) indicate that this level of derepression during a 30-min period (16) may produce a burst of *cro* protein sufficient to completely turn off P_{RM} by ≈ 40 min after the beginning of the inactivation process.

17. Riechardt, L. & Kaiser, A. (1971) *Proc. Natl. Acad. Sci. USA* **68**, 2185–2189.
18. Chadwick, P., Pirrotta, V., Steinberg, R., Hopkins, N. & Ptashne, M. (1973) *Cold Spring Harbor Symp. Quant. Biol.* **35**, 283–294.
19. McGhee, J. D. & von Hippel, P. H. (1974) *J. Mol. Biol.* **86**, 469–481.
20. Schwarz, G. (1977) *Biophys. Chem.* **6**, 65–76.
21. Epstein, I. R. (1978) *Biophys. Chem.* **8**, 327–339.
22. Lee, N. L., Gielow, W. O. & Wallace, R. G. (1981) *Proc. Natl. Acad. Sci. USA* **78**, 752–756.
23. Ogden, S., Haggerty, D., Stoner, C. M., Kolodrubetz, D. & Schleif, R. (1980) *Proc. Natl. Acad. Sci. USA* **77**, 3346–3350.
24. Brent, R. & Ptashne, M. (1980) *Proc. Natl. Acad. Sci. USA* **77**, 1932–1936.
25. Meyers, R. M., Rio, D. C., Robbins, A. K. & Tjian, R. *Cell* **25**, 373–384.
26. Maxam, A. M. & Gilbert, W. (1977) *Proc. Natl. Acad. Sci. USA* **74**, 560–564.
27. Sanger, F. & Coulson, A. R. (1975) *J. Mol. Biol.* **94**, 441–448.
28. Galas, D. J. & Schmitz, A. (1978) *Nucleic Acids Res.* **5**, 3157–3170.